Available online at www.sciencedirect.com

ScienceDirect

materialstoday: PROCEEDINGS

[2022 International Conference on Engineering for a Sustainable World]

Analysis of the morphological and mechanical characterization of aluminium matrix composite reinforced with chitosan

N. E Udoye[a], V Ezekiel[a], O. S. I. Fayomi[c,d], I. P. Okokpujie[b], and J. O. Dirisu[a].

[a]*Department of Mechanical Engineering, College of Engineering, Covenant University Ota, Lagos state, Nigeria*

[b]*Department of Mechanical Engineering, College of Engineering, Afe Babalola University Ado-ekiti, Ekiti State , Nigeria*

[c]*Department of Mechanical and Biomedical Engineering, Bells University of Technology, P.M.B 1015, Ota, Ogun State, Nigeria*

[d]*Department of Chemical, Metallurgical and Materials Engineering, Tshwane University of Technology, P.M.B, X680, Pretoria, South Africa*

Corresponding Author: nduka.udoye@covenantuniversity.edu.ng, +2348035278117

Abstract

Recent studies acknowledge that convectional ceramic particulate could be replaced by several agricultural by-products in the development of aluminium matrix composites because of its selected for their low cost and relative ubiquity. This study explores the development of aluminium matrix composite from AA6061 alloy reinforced with chitosan particulates at weight proportions (3, 6, 9, and 12wt.%). The study further characterizes the developed composites using Scanning Electron Microscopy (SEM), Energy Dispersive Spectroscopy (EDS), X-ray Diffractometer (XRD), hardness, tensile and thermal and electrical conductivity test techniques. Results indicated that increasing chitosan content up to 10 wt. % enhanced the hardness performance, while tensile strength of the composites increased sporadically, as SEM images observed reinforcement links embedded in grain boundaries. However, the thermal and electrical conductivity diminished due to the addition of chitosan particulates to the alloy matrix. The overall study showed the great potential of chitosan polymer as reinforcement to aluminium alloy.

Keywords: AA6061, Chitosan, SEM/EDS, XRD, Thermal, Electrical Property

Nomenclature	
SEM	Scanning Electron Microscopy
EDS	Energy Dispersive Spectroscopy
XRD	X-ray Diffractometer

1. Introduction

The evolution of the engineering discipline has intimated developments of advanced materials to sustain equipment performance in austere conditions confronted in the energy, aerospace, automotive and construction industries. Scientists have purported metal matrix composites MMC for the enhancement of material strength to weight ratio, dilapidation resistance, and conductivity in industrial machinery [1, 2, 3]. Aluminium is a quintessential metal to human civilization. As noted in literature, reinforcements provide material property customization targeted at specific engineering needs. Aluminium, a copious lightweight metal, has been extensively applied in the fabrication of automobiles and aeroplanes parts, components, and structures. Yet, the laudable corrosion resistance, substantial thermal and electrical conductivity of aluminium influence its utilization as base material in household utensils, sporting equipment, appliances, and electronic devices. Thus, extensive research has sought to extend the application of aluminium by improving certain desirable properties. Subsequently, scientist have developed and investigated aluminium matrix composite reinforced with ceramics: Al_2O_3 , aluminium oxide; SiC, silicon carbide SiO_2, silicon

oxide; B_4C, boron carbide; and TIC, titanium carbide. However, the prevalent interest on sustainability and the impact of human activities to the environment highlight pollution produced from the synthesis of ceramic reinforcements. Furthermore, concerns over the availability and cost of aluminium metal matrix composites (AMMCs) reinforced with ceramic composites have limited AMMC adoption at a large scale. Accordingly, cost efficient synthesis technique, most notably stir casting, have been adopted as well as the utilization of agricultural waste material as reinforcement in AMMCs. Therefore, agro–waste like rice husk, breadfruit seed, bagasse seed, eggshell, coconut husk, and aloe vera have gained prominence in industry as preferred alternatives to ceramic reinforcements, moreover numerous research work is dedicated to exploring reinforcement materials to attain superior corrosion, mechanical and morphological properties to that of unreinforced aluminium. These waste derivatives of terrestrial and aquatic animals as well as plants have been found to attenuate environmental impact and improve material performance. Hence, this research seeks to employ chitosan particulates of 90 microns sieve size as reinforcement to the AA6061 aluminium alloy matrix developed via stir casting and characterize the composites mechanical, morphological, thermal, and electrical properties.

2. Literature Review

2.1 Ceramic reinforcements of aluminium alloys

Reinforcement of metals to achieve superior performance predates modern civilization [4, 5] , however preliminarily contemporary applications of aluminium composites were in the development of aircrafts [6]. Driven, Over the years, scientists have explored reinforcement materials particularly ceramic particulates in developing AMMCs. The ceramic particulate, alumina, Al_2O_3, is highly prioritized in reinforcements selection for aluminium and its alloys, which is attributed to empirically proven superiority in hardness, tensile and stiffness properties of aluminium matrix composites composite Al_2O_3 [7]. The analyzed impact resistance of squeeze cast alumina reinforced AC-44200 further emphasizes the advantage of reinforcing aluminium alloy in alumina, when [8] appraised ballistic resistance of the unreinforced alloy and the developed composite. The authors discovered that the aluminium alloy with 20 and 40 per cent alumina by volume effectively dissipated 30 % and 50 % impact energy causing a significant retardation in projectile velocity. This interesting discovery proved relevant as ballistic shield would experience a significant reduction in weight to effectiveness in military armours. Subsequently, an investigation of the mechanical and morphological effects of AA6061 reinforcement with hybrid particulates consisting of boron nitride and alumina. [9] demonstrated an improvement in mechanical strength of the alloy. Increasing BN proportions in the composites led to significant improvements in compressive, impact, hardness, and tensile strengths. The authors further noted enhanced dilapidation resistance of wear and corrosive conditions in developed composite. Likewise, ceramics like silicon carbide have been explored by researchers as reinforcements for aluminium, metal or alloy, matrix. Heat dissipation performance being critical in aircrafts and automobiles, [10] examined the as cylindrical fins for various ceramic fillers, of AA 6061 matrix. The authors found most significant improvement in thermal dissipation properties, conductivity and heat transfer coefficient correspondingly greater in composites reinforced with boron nitride, alumina, and silicon carbide over the as-cast AA 6061 alloy. Such Improvements are largely attributed to quantities of newly formed phases like Fe_2SiAl_8 and $Al_{15}(Fe,Mn)_3Si$ dispersed within the previous vastly mono-atomic matrix [11]. However, [12] noted that with increased presence of diamond in the hybrid reinforcements, silicon carbide + diamond, thermal and electrical conductivity of the aluminium composite. confirmed this to be the detrimental effect of Silicon precipitate phases in the composite and prolonged contact of silicon and molten aluminium matrix as observed in composite manufactured with pressure infiltration fabrication technique. Thus, the introduced diamond ensured less silicon availability for dissolution. Furthermore, titanium carbide reinforcements of AA 6061 in in-situ reaction with both silicon carbide and k_2TiF_6 expressed with evenly dispersed TiC particulates and precipitated intermetallic phases over the standard alloy were formed in [13]. The authors further noted an almost linear improvement in hardness, UTS and percentage elongation with increasing TiC presence. More recently, [14] found graphite–titanium carbide hybrid reinforcement of aluminium in varying weight proportions showed enhanced wear resistance over unreinforced alloy. The 4 wt. % TiC sample exhibited highest hardness and tensile strength gains over AA 7075. Finally, [15]examined behaviours of various ceramic particulate reinforcements in AA 7075. They studied reinforcing addition of 15 wt. % of Al_2O_3, SiC, B_4C and TiB_2. The authors discovered maximum improvements in hardness, tensile, impact strength performance of composites over as-cast alloy in the B_4C reinforced sample. Thus, they endorsed the selection of B_4C particulates for customized aluminium alloy improvements in mechanical behaviour.

2.2 Agricultural waste reinforcements of aluminium

Recently, metallurgy research has focused on reinforcements of aluminium matrix composite with agricultural waste materials. While being economical, these waste materials undergo value recycling satisfying the modern concerns on sustainability and ecological impact of manufacturing activities. However, extensive investigations are conducted to compare the performance gains of these composites and the properties of unreinforced aluminium alloys, as well as AMMCs, reinforced with conventional materials (i.e., ceramics).

2.2.1 Wood

Significant quantities of wood have been used throughout civilization in the construction of roads, bridges, and buildings [16]. However, one of man's most renewable, now facing shortage, has inspired researchers and environmentalists to continually explore the sustainable application of organic fibre in engineering materials such as aluminium composites [17, 18]. The results of this research bring ecological preservation worldwide and economic gains to developing cities and countries with substantial housing problems. The synthesis of waste wood particulate reinforced aluminium reinforced in [19] experienced decreased density with the addition of reinforcements. The authors also noted that 97.69 MPa ultimate tensile in 20 wt. % wood reinforced aluminium matrix composite and 89.4 % greater impact strength values in 10 % wood reinforced aluminium composite compared to unreinforced aluminium alloy derived from crushed cans.

2.2.2 Egg shells

Presently, numerous tons of eggshells are included as a calcium supplement in livestock feed [20]. Furthermore, Egg shells are currently utilized in absorbent heavy metals in industrial wastewater through climate action programs [21]. The relative ubiquity of poultry industries worldwide justifies the exploration of eggshells as potential reinforcement material [22]. More so, [23] examination of the effects of uniformly dispersed carbonized and uncarbonized eggshell reinforcement in Al-Cu-Mg show increased tensile strength and hardness of the alloy attributed to improved dislocation density caused by the hard eggshell phase. Furthermore, [24] appraised the mechanical properties of chicken eggshell particulates in AA 2014. The resulting composite showed enhanced fatigue and tensile strengths while maintaining low porosity and uniform dispersion of particulates in the alloy matrix. Thus, researchers in [25] combined ball-milled eggshells and alumina in hybrid reinforcements of heat-treated aluminium hybrid composite. The resulting composite provided significantly impressive harness and tensile strength performances over aluminium-egg shells and aluminium-alumina composites. Also, improvements in corrosion resistance transpired with the addition of alumina-eggshell reinforcement.

2.2.2 Coconut husk ash

Cocos Nucifera (Coconut) fruit consists of the liquid endocarp, solid endocarp, mesocarp and exocarp [26]. The liquid endocarp, coconut milk, is consumed or processed industrially into beverages, while the endocarp is processed into creams and pharmaceuticals [27]. However, the mesocarp, shell, of coconut is generally incinerated or disposed of as waste. With rising oil and gas prices, developing countries synthesize coconut shells into biofuel mixtures to meet energy needs [28]. Crop cultivators use CSA to stabilize poor laterite soil as well as fertilizer additive [29, 22]. Similarly, wastewater treatment systems can apply to activate carbon-based absorbent produced from coconut husk for the removal of dyes [30]. Recently, the ash of coconut husk has been identified to contain up to 90% silica. Thus green silica synthesis techniques have been developed to attenuate the adverse ecological impact of industrial synthesis of silica by a series of heat and acid treatments of coconut husk [31]. Therefore, the ash has undergone studies as a secondary reinforcement in AMMCs and an alternative to ceramics for composite development. [32] reinforced AA6061 with coconut shell ash - SiC mixture using stir casting process in an effort to complement synthetic convention reinforcement, carbide particulates, with agricultural waste coconut shell in composite formation. The developed composite showed improved hardness in the Vickers hardness tester over the as-cast alloy. Also, the coconut shell composite expressed higher % elongation, yield strength and tensile strength properties than the base alloy. [33] investigated the effects of B4C and coconut husk ash reinforcement on mechanical characteristics of aluminium 7075. Results show that increasing B4C – CSFA particulate in the alloy increased hardness and enhanced the tensile strength with an observed maximum at 12 wt. % B4C – CSFA reinforcement. [34] identified enhanced Grey-Fuzzy reasoning grade wear performance on aluminium composite with the increasing volume of coconut shell ash fabricate via compo-casting technique.

2.2.4 Rice husk ash

Rice husk (RH) is a silica-rich outer membrane of the rice crop [35]. The crop widely grown worldwide in paddies is a primary agricultural product. The husk, a by-product of the milled rice crop, is traditionally used as a fuel and in

cement production. Because the ash contains 90 % amorphous silica content [36, 37], numerous industrial applications employ it as a natural silica alternative. Silicon oxide and Silicon carbide are themselves good ceramic reinforcements for AMCs. Thus, rice husk ash is a common agricultural waste reinforcement material. For example, [38] compo-casted aluminium matrix composites using rice husk ash of varying weight proportions as reinforcement. The authors found that increasing proportions of RHA yielded higher hardness and wear resistance properties of the composite. Thus, mixture with NaOH, heating, dilution of mixture with DI water, titration and gelatinating; is a significant portion of the Taungchi RHA silica extraction method [39]. A unique benefit economically to industry seeking to increase production output of high-performing AMCs at a reduced cost. Although acid or alkaline treatment of RHA increases silica purity of the product [35], unprocessed ash, a product of combustion in a boiler, would have served as an energy source and contained as much as 95 % silica. Also, [40] evaluated using XRD, the crystallinity of pyretic RHA (at up to 1000°C) was 88.6 %. Further studies on RHA as reinforcement show up to a 12 % increase in the ultimate tensile strength of AlSi10Mg [41]. In the investigation of mechanical, morphological and topological properties of AlSi10Mg reinforced with RHA fabricated via powder metallurgy, [42] discovered that the maximum hardness of the composite at 10 wt. % RHA reinforcement was over 15 % greater than that of the unreinforced aluminium. In addition, the authors observed a reduced wear loss using pin-on-disc apparatus on the 5, 10, and 15 wt. % RHA reinforced samples. The Signal to Noise ratio, larger, is better, statistically evaluation of AA6063/10 wt. % weldments fabricated through the stir casting route show sound weldment response to varying welding speed, current and gas flow rate parameters [43]. The varying parameters yielded consistently increasing tensile and impact strengths of weldments. Thus, the authors suggested aerospace application of the composite due to its lower density, good weldability and joint strength for fabrication using the TIG welding process. Similarly, Friction stir casting of AA6061/RHA provided even dispersion within the alloy matrix observed through FESEM and strong interfacial bonding between RHA particles and the aluminium alloy, resulting in enhanced tensile strength of the alloy [44]. It can be concluded that rice husk ash performance, ubiquity, and low cost of the ash is a waste material evidently cements as a viable alternative to SiC and SiO2 in composite development.

3. Experimentation

3.1 Material

The materials selected for this research are AA6061 and Chitosan particles of sieve size 90μm.

3.2 Preparation of Aluminium Matrix composite

In this study, stir casting is employed for the development of composites. Stir casting involves the use of a mechanical stirrer to consolidate reinforcement particulates in a molten metal by creating forced vortexes. The process ensures the homogeneous distribution of the particulates in the base matrix. Thus, obtained chitosan particles were sun-dried and milled to smooth powder, as shown in Figure 1a. The particles are then sintered. AA6061 was heated to liquefaction and placed in a crucible. A mixture of molten AA6061 and sintered chitosan powder are stirred vigorously at about 500rpm [45]. The mixture is then transferred into pre-heated dies and allowed to solidify at room temperature to reveal the AA6061/chitosan castings. Figure 1b shows images of developed aluminium matrix composites.

Fig. 16a: Dried Chitosan Powder

Fig. 16b: Cast aluminium matrix composites

3.1 X-ray diffraction analysis

X-ray diffraction analysis provides the qualitative crystallographic of the developed samples. Thus, the various composing lattice-structured compounds are identified. XRD technique involves the use of monochromatic collimated X-ray beam incident on sample resulting in scattering of X-rays on interaction with atoms and molecules of the material. These scattered X-rays are diffracted at disparate angles, which are effects of constructive interference between constituting particles of the sample and the incident rays. Characterization of composing phases is obtained by analysis of the various diffraction angles using Bragg's law given in Equation 1. Moving detector and goniometer pair are used to identify x-rays and measure diffraction angles, respectively. The counter is used to record the count rate of the observed radiation.

$$n\lambda = 2D\sin(\theta) \tag{1}$$

where, d is the wavelength λ is the

wavelength n is the order of the

diffraction θ is the angle of

diffraction in degrees

3.4 Coconut husk ash

The developed composites were subjected to the Brinell hardness test to obtain the hardness. The tester provides precise hardness values using Brinell's technique that accommodates uneven surfaces better than other tests. The samples were tested with a load of 300 Kgf applied to a 10 mm ball indenter at a mass of 100 g for over 15 seconds. The resulting indentations are observed and measured using a Brinell microscope to obtain the diameter of the pit. Then, indentation diameters are then averaged out to surface inconsistencies.

$$BHN = \frac{2P}{\pi D(D - \sqrt{D^2 - d^2})} \tag{2}$$

where,

P = load applied (KN)

I = diameter of indenter (mm^2)

R = Resistance in indenter (mm^2)

3.5 Tensile tester

Tensile properties of the cast composites are tested using the UTM SM1000 Tensile tester. The tester is employed to evaluate the tensile strength, yield strength and elongation characteristics of the samples. The instrument used load cells of 100 kN on the 10 mm composite samples. By placing the fabricated samples between the machine holds, the tester is able to evaluate the tensile strength by the ASTM A370 standard.

3.6 Scanning Electron Microscope

Morphological imaging was done using a Scanning Electron Microscope. This optical imaging technique provides adequate details on the grain arrangement, sizing, boundary, and faults. For the test, the sample surfaces were polished using an emery board. The scanning electron microscope uses a focused beam of electrons to provide optical data on the surface microstructural of the samples. The microscope was configured to 15 KV, acceleration voltage; 20 μ m, working distance; and between 30000 to 35000x magnifications. The resulting images are printed onto a micrograph with dimensional reference included.

3.7 Thermal and Electrical Conductivity test

The thermal and electrical conductivity of the samples were evaluated using separate testing techniques. Electrical conductivity and resistivity values for the as-cast alloy and developed composites were estimated using the ammeter-voltmeter method. Here, a 5A-ammeter is connected in series with a voltage source, while the voltmeter is connected across the samples, as shown in Figure 1.3. DC supply voltage is applied in steps of 0.2V. The resulting current values are measured and tabulated to obtain the mean electrical resistance through linear regression. Hence, the electrical resistivity and conductivity can be estimated using equations Equation 3, Equation 4 and Equation 5. Thermal conductivity was evaluated from temperature, humidity and air velocity parameters of forced convection under greenhouse conditions. A digital hygrometer, Lutron HT-3003, with a least count of 0.1 %, was utilized to quantify the relative humidity within the greenhouse. Similarly, a digital hygro-thermometer (model: Lutron HT-3003) with the least count of 0.1 % was used to measure the relative humidity inside the lab while weighing the samples. The test setup required evaluation of the air properties within the greenhouse. Thus, an electronic anemometer determines the air velocity across the section of the greenhouse. Raytek MT-4 non-contact thermometers measured the temperature on the surface of the composite samples.

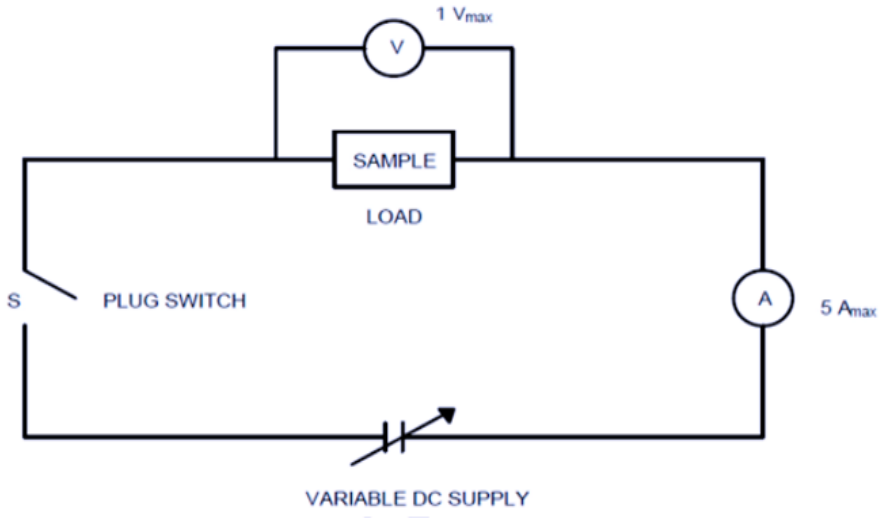

Fig. 2: Electrical properties test circuitry

$$Resistance, \quad R = \frac{V}{I} \tag{3}$$

$$Resistivity, \quad \rho = \frac{R * A}{l} \tag{4}$$

$$Conductivity, \quad G = \frac{1}{\rho}$$

(5)

where
V = Voltage in V (Volts)
I = Current in A (Ampere)
R = Resistance in Ω(Ohms)
ρ = Resistivity in Ω-m (Ohm-meter)
G = conductivity in S/m (Siemen per meter)
A = Area in m^2 (square-meter)

4.1 X-ray Diffraction Analysis

The diffractogram pattern was generated using a Cu-Kα powder X-ray Diffractometer, Rigaku D/Max-111C, with a Braggs 2θ scale from 10°to 45°. Figure 3 illustrates the XRD pattern of AA6061 + 0 wt.% Chitosan. The diffractogram of unreinforced alloy reveals peaks of major $Ca_2Al_3SIO_4$, $CaCO_3$, Ca_2SIO_4, and $Ca(OH)_2$, indicating a contaminated alloy with the elevated elemental presence of Ca. AA6061 + 3wt.%. 3 wt.% Chitosan reinforced sample generates an XRD pattern with observed peaks with that of the unreinforced alloy. Nevertheless, the pattern includes hydroxyapatite, $Ca_{10}(PO_4)_6(OH)_2$. Result patterns in Figure 5, Figure 6, and Figure 7 are suggestive of the presence of the $Ca_{10}(PO_4)_6(OH)_2$ biogenic compound in developed composite with 6, 9 and 12 wt.% Chitosan respectively. The patterns are observed to increase hydroxyapatite phase intensities with rising weight proportions of agro-waste, Chitosan. The numerous occurrences of hydroxyapatite, $Ca_2Al_3SIO_4$ and other phases in the XRD data substantiates evidence of organic matter convoluted in alloy matrix during composite coalescence.

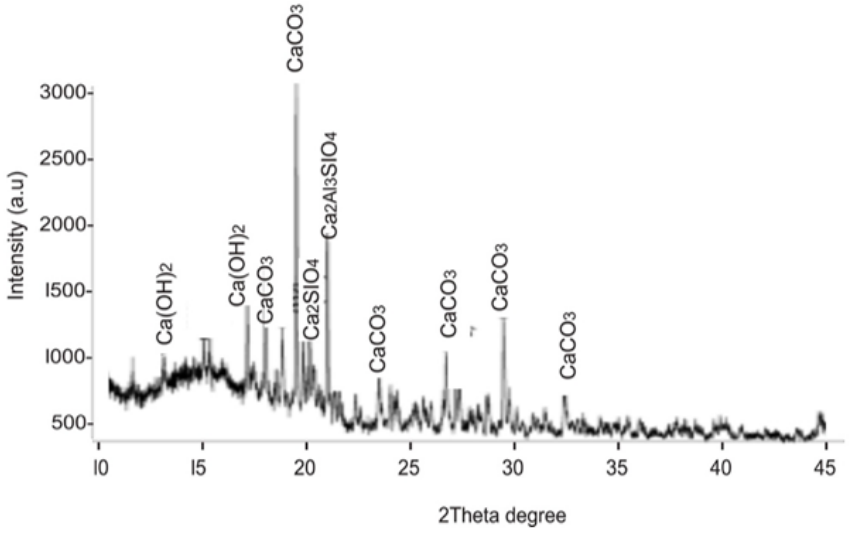

Fig. 3: XRD pattern of as-cast AA6061

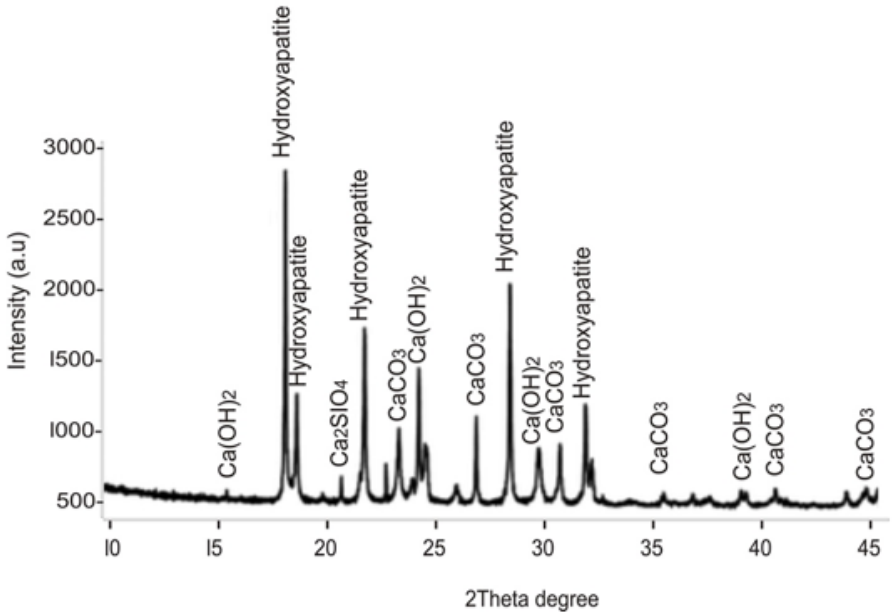

Fig. 4: XRD pattern of AA6061 + 3wt.% chitosan

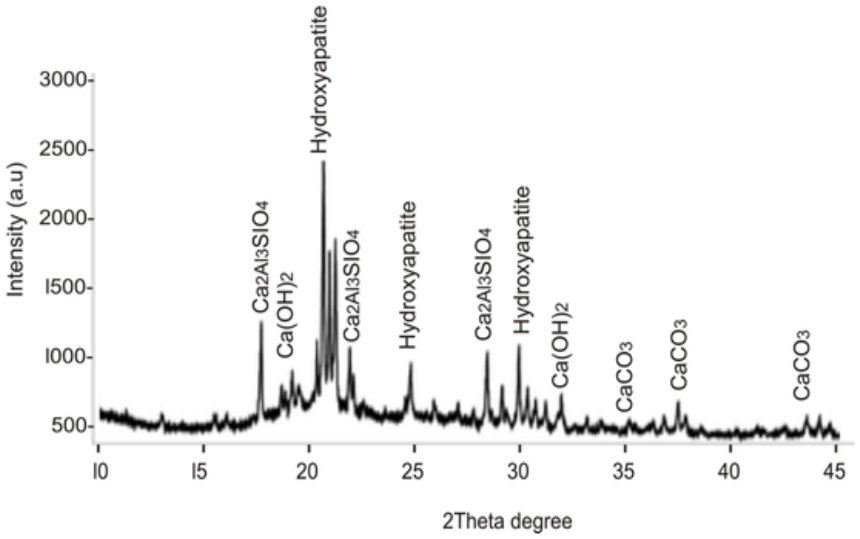

Fig. 5: XRD pattern of AA6061 + 6 wt.% chitosan

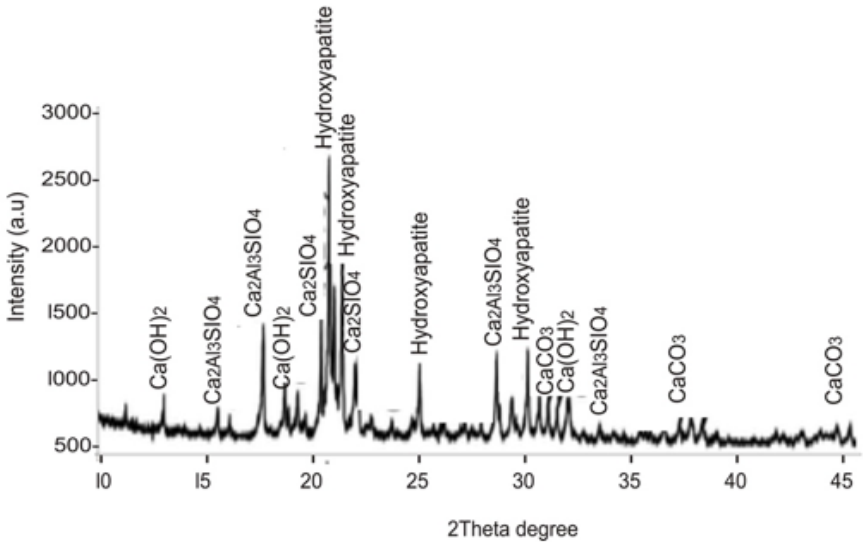

Fig. 6: XRD pattern of 9 wt.% chitosan

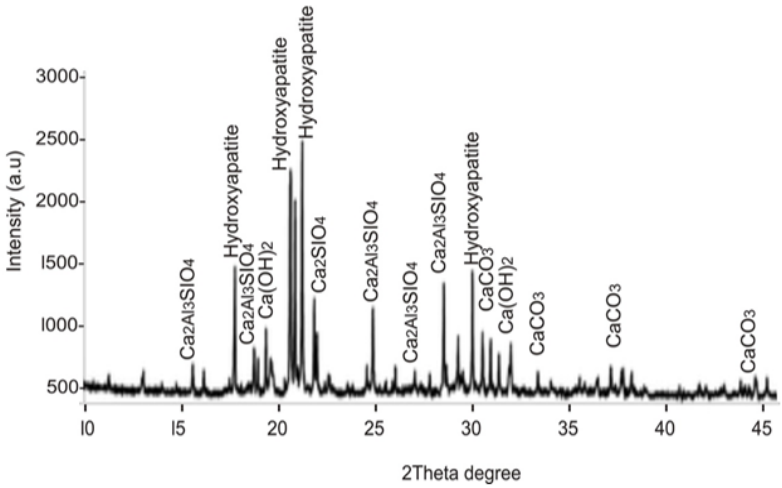

Fig. 7: XRD pattern of 12 wt.% chitosan

4.2 Mechanical Properties

Mechanical characterization of chitosan reinforced composites performed using SM1000 tensile tester is demonstrated in Figure 8 and Figure 9, respectively. The maximum percentage elongation at ultimate tensile strength (UTS) was 2.334 % for the unreinforced alloy, which declined with the addition of chitosan reinforcement. Figure 8 depicts reduced strain at UTS as the weight proportion of chitosan reinforcements increased in the alloy matrix. Nevertheless, tensile strength is enhanced sporadically with higher weight proportions of chitosan reinforcement. Hence, 12wt. % chitosan possessed the highest ultimate tensile strength of 114.92 MPa; a 38.4 % increase in the mechanical property, as seen in Figure 9. Similarly, evaluations carried out using Brinell's hardness tester indicate sporadic improvements in hardness, as illustrated in Figure 10. The highest harness, 60.2 HRB observed in 9 wt. % chitosan reinforced sample indicated a 4.88 % improvement over as-cast AA6061 hardness (57.4 HRB). However, hardness perceptibly declined with more chitosan reinforcement. Yet, 3 wt.% and 6 wt.% chitosan reinforced AA6061 developed higher resistance to local deformation, 59.2 HRB and 57.8 HRB, than the unreinforced alloy. Results show insufficient improvement in aluminium matrix composite reinforced with 6 wt.% chitosan over 3 wt.% chitosan.

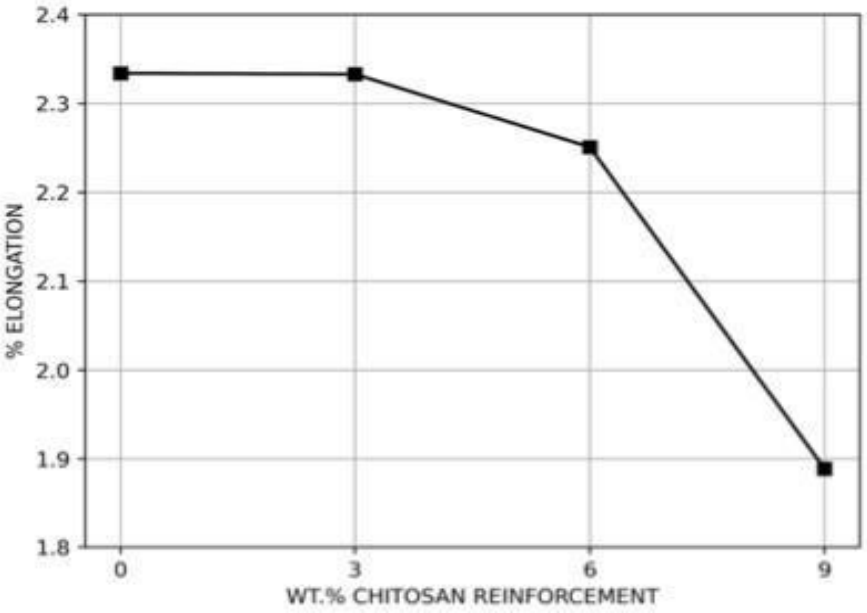

Fig. 8: % elongation of aluminium matrix composites

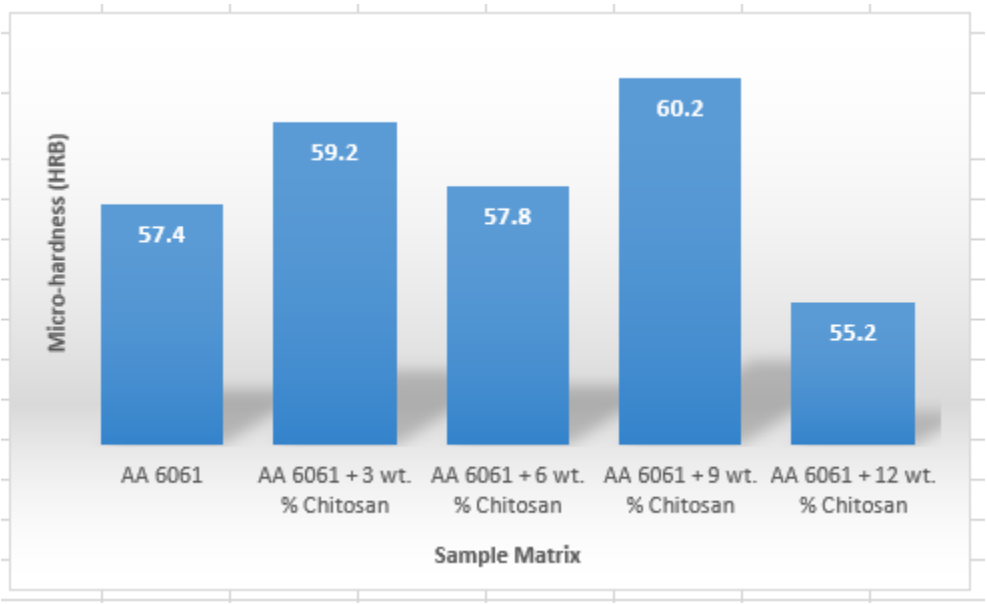

Fig. 9: Hardness of aluminium matrix composites

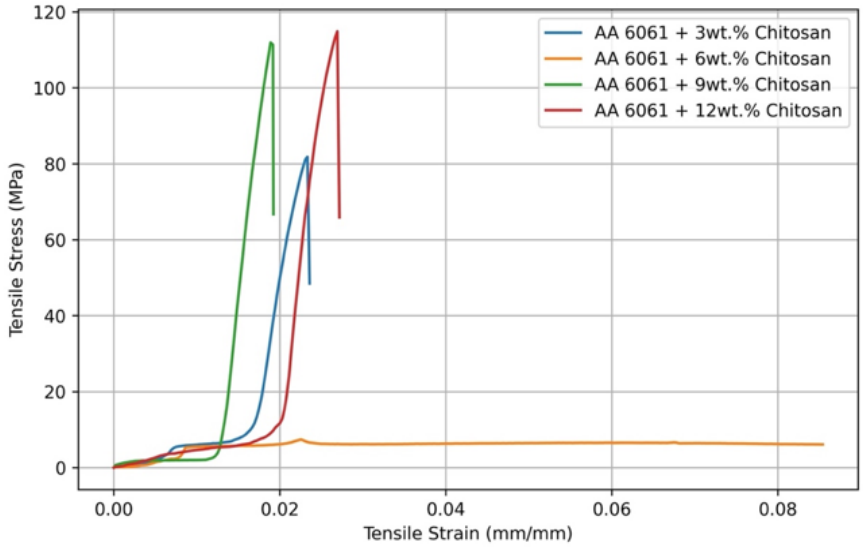

Fig. 10: Tensile Strength of aluminium matrix composite

4.3 Mechanical Properties

The electrical conductivity of aluminium varies considerably between 30 S/m and 65 S/m, depending upon the metal's chemical composition and physical properties [46, 47]. Figure 11 shows the non-linear trend in electrical conductivity for the synthesized aluminium matrix composites. The evaluated electrical conductivity is maximum at 38.20 S/m for 12wt.% reinforced aluminium composite, while conductivity decrease is observed in 0, 3, 6, 9 wt.% samples with values 37.81, 36.21, 36.61, 35.49 S/m. A marginal rise occurred in 6 wt.% chitosan reinforced sample. However, it represented no improvements to the conductivity of unreinforced alloy. An analogously inverse trend is established in Figure 12 where electrical resistivity peaks at 0.028 ωm in 9 wt.% chitosan reinforced sample, followed by a decrease for the 12 wt.% chitosan sample, 0.026 ωm. Thus, further research should be carried out on aluminium alloy AA 6061, reinforced with chitosan of weight proportions above 12% to attain substantial improvements in electrical conductivity.

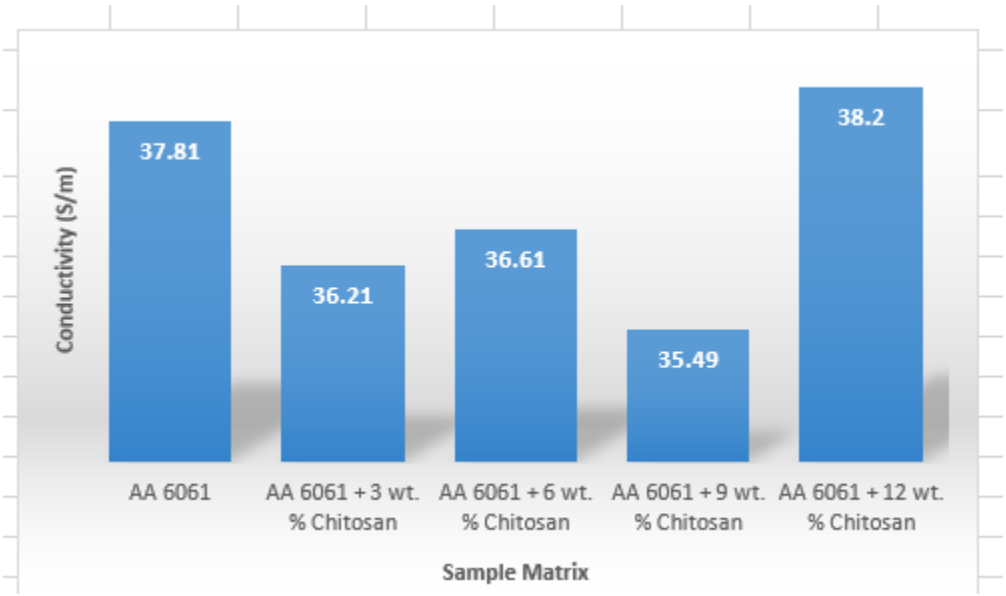

Fig. 11: Conductivity of aluminium matrix composites

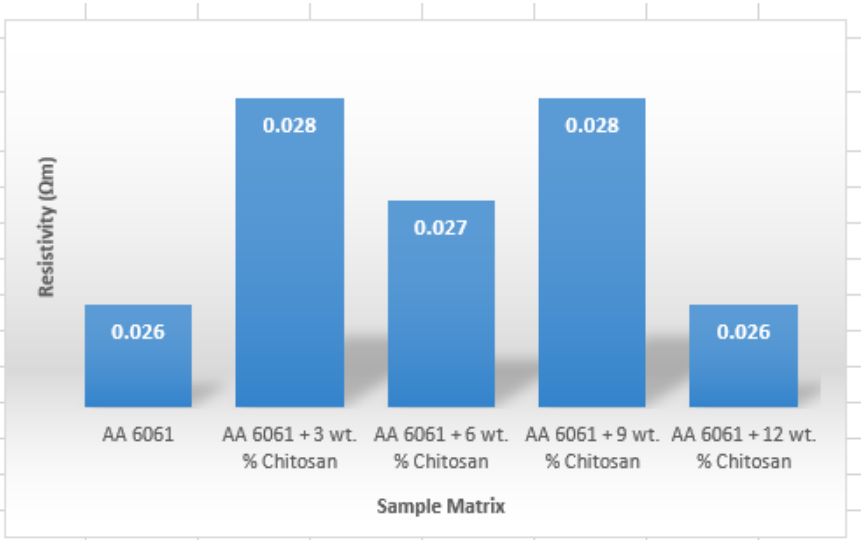

Fig. 12: Resistivity of aluminium matrix composites

The heat transfer coefficient is an important thermal property in the selection of materials for industrial use. In Figure 13, the conductive heat transfer coefficient is represented for unreinforced alloy and each of the developed composites. The calculated mean heat transfer coefficient for the composites reinforced with 3, 6, 9, and 12 wt.% chitosan increased with the increasing weight proportions from 124.16 to 189.40 W/m°C, as seen in Table 1. However, adding chitosan failed to improve the overall thermal conductivity of the unreinforced alloy AA6061, which was obtained as 362.97 W/m°C. Thus, while the reinforcement reduced the thermal contact resistance between grains in the alloy matrix, its composition of silicon, calcium, and oxygen, which are majorly poor thermal conductors with low thermal conductivity, resulted in an overall thermal conductivity decrease. Similarly, results obtained from the addition of graphite-silicon carbide to aluminium alloy show lower thermal conductivity with added hybrid reinforcement of high silicon content compared to that of the as-cast alloy [48]. Therefore, the reinforcement resulted in increased density of alloy matrix structure, limiting the flow of electrons. The results obtain still show high thermal conductivity for the AA6061- chitosan composite, which is suitable for electronic packaging requiring heat management, such as fins for microprocessor units in computers.

Table 1: Heat transfer coefficient of aluminium matrix composites

Sample	Conductive Heat Transfer Coefficient (W/mK)
AA 6061	362.97
AA 6061 + 3 wt.% Chitosan	141.59
AA 6061 + 6 wt.% Chitosan	189.40
AA 6061 + 9 wt.% Chitosan	141.59
AA 6061 + 12 wt.% Chitosan	124.16

4.4 SEM/EDS analysis

Morphological characterization of aluminium was obtained using Scanning Electron Microscopy (SEM) and Energy Dispersive Spectroscopy (EDS) techniques. Figure 14a and Figure 14b show microscopic and compositional data on the unreinforced AA6061 aluminium alloy, the sample obtained through SEM and EDS, respectively. As observed in Figure 15a, 0.2 μm sized fibrous particulates of the 3 wt.% chitosan reinforcements surround the darker well-defined alloy matrix seen in Figure 14a. Minimal voids of approximately 10 μm are observed in the composite structure.

Compositionally, the EDS result, Figure 15b, of the composite showed increased calcium and oxygen contents of the composite, indicating intrinsic. In contrast, this indicates stirred, both of which are found abundantly in the chitosan reinforcement. From Figure Figure 16a, near-perfect dispersion of chitosan forms a link structure that occupies most of the grain boundary. This serves to distribute load and improves the tensile performance of the composite. EDS analysis shows distinguishable growth in the percentage of calcium and oxygen elements in the composite. A result of more chitosan constituents to convolute with intermetallic phases of the alloy matrix.

The 9 wt.% chitosan reinforced composite morphology observed in Figure 17a shows the meticulously arranged composite structure previously observed in Figure 15a and Figure 16a. However, more chitosan particulate innocuously occupies grain boundary voids in even distribution, as observed in Figure 17a resulting in a higher load-bearing capacity. Thus, a further improved mechanical performance is observed from the composite mechanical characterization. EDS data show rising oxygen content partly responsible for its electrical resistance with pronounced Silicon, Iron, Carbon and Magnesium constituents. The SEM image illustrated in Figure 18a show a slight agglomeration produced during the composite synthesis of the 12 wt.% chitosan and aluminium alloy. Reinforcements appear to be laid along boundary voids of alloy structure to connect adjacent grains of the continuous matrix. The EDS analysis, Figure 18b, identifies prominent calcium and oxygen peaks and highlights the rising elemental carbon composition indicating rich biogenic material presence within the composite.

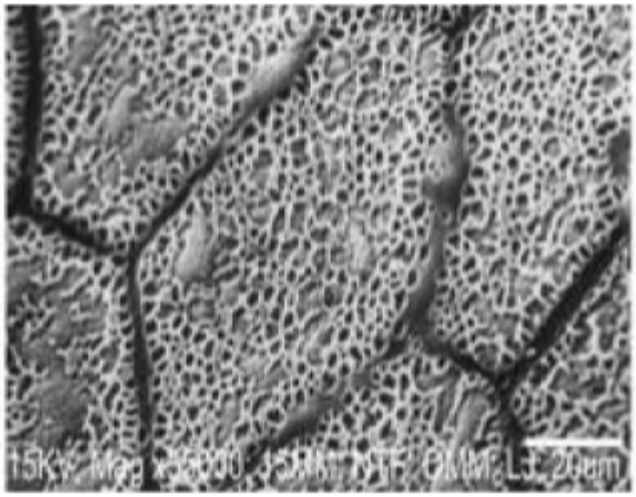

Fig. 14a: SEM image of unreinforced AA6061 sample

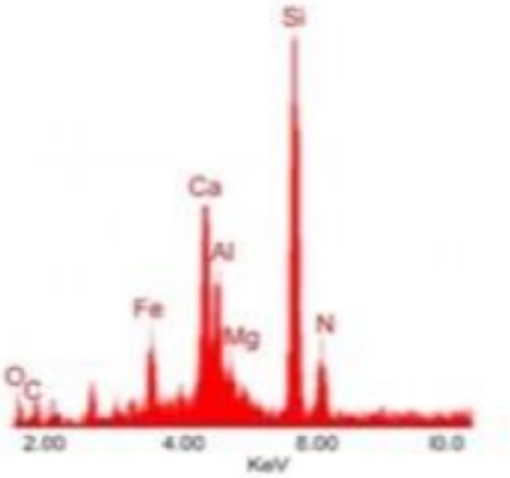

Fig. 14b: EDS of sample

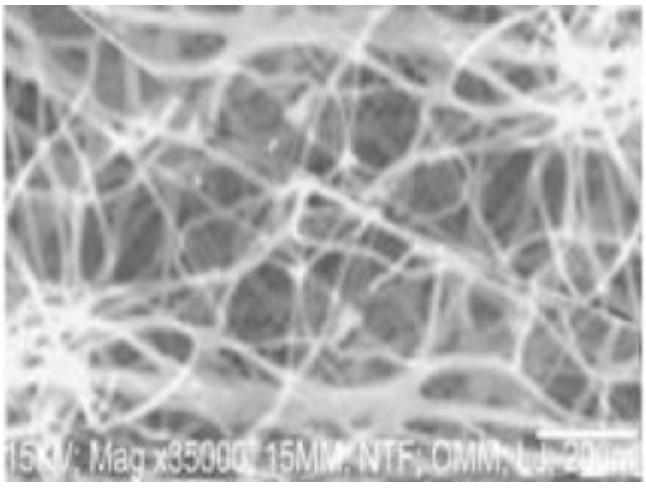

Fig. 15a: SEM image of 3 wt.% chitosan reinforced AA6061 sample

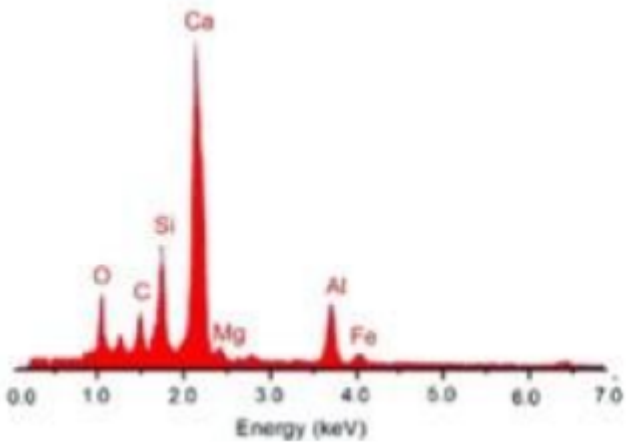

Fig. 15b: EDS of sample

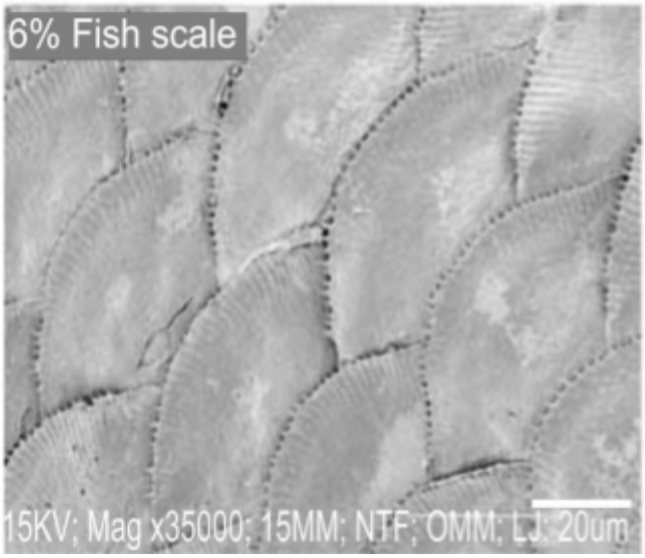

Fig. 16a: SEM image of 6 wt.% chitosan reinforced AA6061 sample

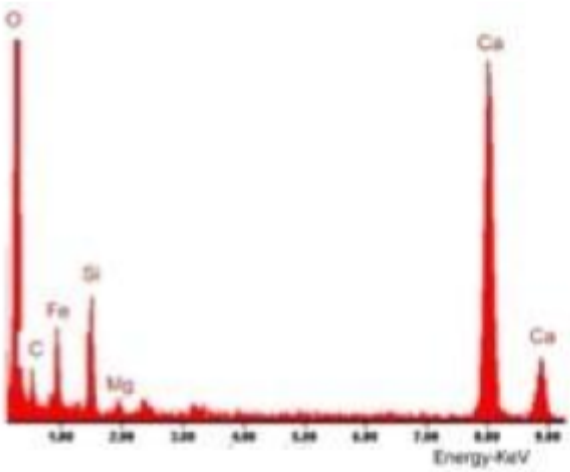

Fig. 16b: EDS of sample

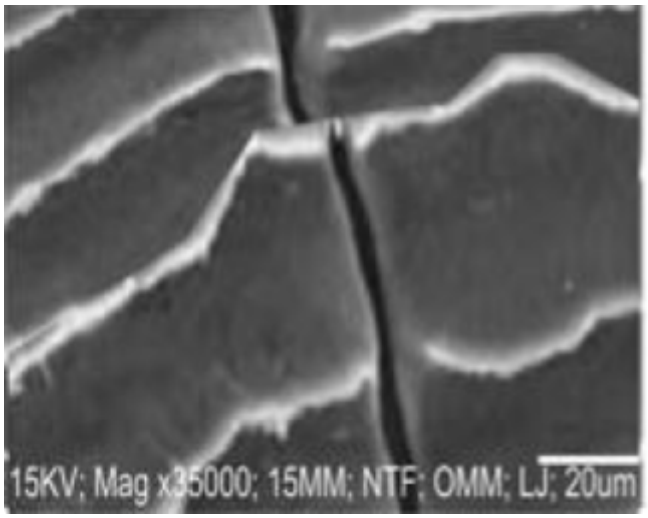

Fig. 17a: SEM image of 9 wt.% chitosan reinforced AA6061 sample

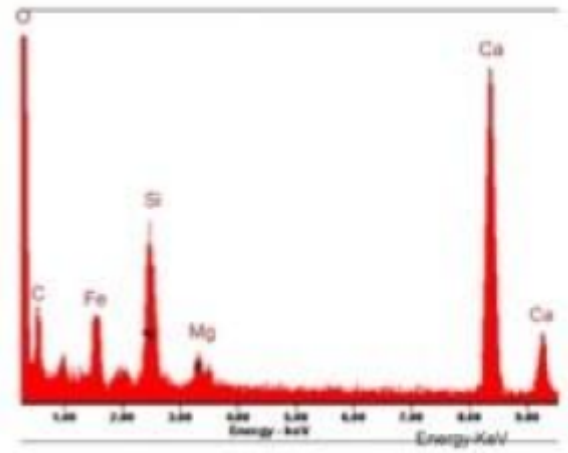

Fig. 17b: EDS of sample

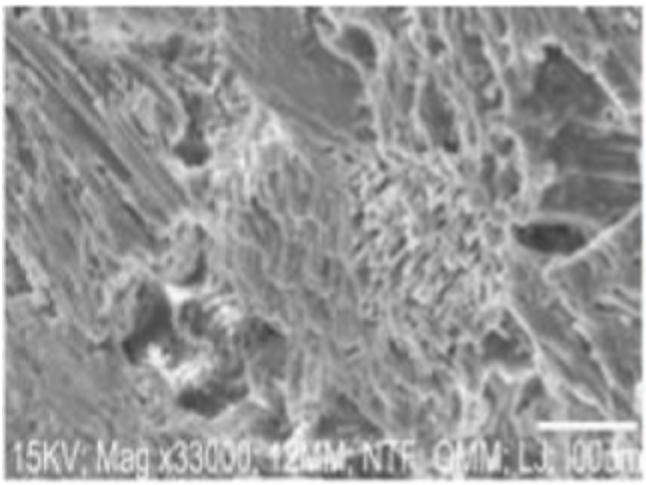

Fig. 18a: SEM image of 6 wt.% chitosan reinforced AA6061 sample

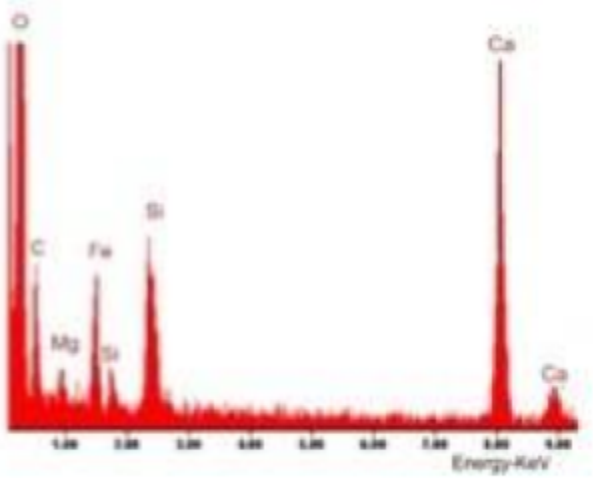

Fig. 18b: EDS of sample

5. Conclusion

Chitosan of 90 microns sieve-size was successfully coalesced in aluminium alloy, AA 6061, matrix via stir casting in weight proportion 3 %, 6 %, 9 % and 12 %. The characterization of the developed composites resulted in the following conclusions:

- Hardness of the developed composites improved with higher concentration of chitosan particulate; 9 wt.% chitosan reinforced sample developed a substantial 4.88 % improvement.
- Composite coalesced with Particulate Reinforcement high percentage of contained carbon and oxygen, and as well as biogenic phase hydroxyapatite.
- Reinforcement particles were evenly dispersed in alloy matrix with slight agglomeration observed in the 12 wt.% chitosan reinforced sample.

- The electrical conductivity of aluminium matrix composite reinforced with chitosan was reduced compared to unreinforced AA6061 because of the introduction of insulation from chitosan reinforcement.
- The synthesized composites showed enhanced tensile strength performance with a 25.8 % increase observed the 12 wt.% chitosan reinforced sample.
- Stir casted AA6061/chitosan provided reduced conductive heat transfer coefficient compared to as-cast AA 6061.

Declaration of Competing Interest

The authors declare that they have no known competing financial interests or personal relationships that could have appeared to influence the work reported in this paper.

Data Availability

The data used to support the findings of this study are included within the article.

Acknowledgement

This work is based on research conducted at the mechanical engineering department in Covenant University, Ota, Ogun State, Nigeria.

References

[1] Muhammad Mansoor, Muhammad Shahid, Muhammad Mansoor, and Muhammad Shahid. Carbon nanotube-reinforced aluminum composite produced by induction melting. *Journal of applied research and technology*, 14(4):215–224, 8 2016.

[2] T. A. Orhadahwe, O. O. Ajide, A. A. Adeleke, and P. P. Ikubanni. A review on primary synthesis and secondary treatment of aluminium matrix composites. *Arab Journal of Basic and Applied Sciences*, 27(1):389–405, 2020.

[3] P.B. Pawar, R.M. Wabale, and A.A. Utpat. A comprehensive study of aluminum based metal matrix composites: Challenges and opportunities. *Materials Today: Proceedings*, 5(11, Part 3):23937–23944, 2018.

[4] Krishan K. Chawla. *Composite materials: Science and engineering, third edition*. Springer, New York, 2012.

[5] Nikos Tsangarakis. The Notch-Fatigue Behavior of an Aluminum Composite Reinforced Unidirectionally with Silicon Carbide Fiber. *Journal of Composite Materials*, 21(11):1008–1016, 1987.

[6] F.J. Lino Alves, A.M. Baptista, and A.T. Marques. Metal and ceramic matrix composites in aerospace engineering. In Sohel Rana and Raul Fangueiro, editors, *Advanced Composite Materials for Aerospace Engineering*, pages 59–99. Woodhead Publishing, 2016.

[7] Puneet Bansal and Lokesh Upadhyay. Experimental investigations to study tool wear during turning of alumina reinforced aluminium composite. *Procedia Engineering*, 51(NUiCONE 2012):818–827, 2013.

[8] Adam Kurzawa, Dariusz Pyka, Krzysztof Jamroziak, Miroslaw Bocian, Piotr Kotowski, and Pawel Widomski. Analysis of ballistic resistance of composites based on en ac-44200 aluminum alloy reinforced with al2o3 particles. *Composite Structures*, 201(August 2017):834–844, 2018.

[9] S. Gopinath, M. Prince, and G. R. Raghav. Enhancing the mechanical, wear and corrosion behaviour of stir casted aluminium 6061 hybrid composites through the incorporation of boron nitride and aluminium oxide particles. *Materials Research Express*, 7(1), 2020.

[10] A Manivannan, R Sasikumar, R Joshuva, and Durai Singh. Thermal investigation of aa 6061 based particulate metal matrix composites. *International Journal of Mechanical And Production Engineering*, 5(12):2321–2071, 2017.

[11] Durbadal Mandal and Srinath Viswanathan. Effect of heat treatment on microstructure and interface of sic particle reinforced 2124 al matrix composite. *Materials Characterization*, 85:73–81, 2013.

[12] J.-M. Molina, M. Rhˆeme, J. Carron, and L. Weber. Thermal conductivity of aluminum matrix composites reinforced with mixtures of diamond and sic particles. *Scripta Materialia*, 58(5):393–396, 2008. Viewpoint set no. 43 “Friction stir processing”.

[13] K. Jeshurun Lijay, J. David Raja Selvam, I. Dinaharan, and S. J. Vijay. Microstructure and mechanical properties characterization of AA6061/TIC aluminum matrix composites synthesized by in situ reaction of silicon carbide and potassium fluotitanate. *Transactions of Nonferrous Metals Society of China (English Edition)*, 26(7):1791–1800, 2016.

[14] R. Ashok Kumar, A. Devaraju, and S. Arunkumar. Experimental investigation on mechanical behaviour and wear parameters of TIC and graphite reinforced aluminium hybrid composites. volume 5, pages 14244– 14251. Elsevier Ltd, 2018.

[15] Din Bandhu, Ashish Thakur, Rajesh Purohit, Rajesh Kumar Verma, and Kumar Abhishek. Characterization & evaluation of al7075 mmcs reinforced with ceramic particulates and influence of age hardening on their tensile behavior. *Journal of Mechanical Science and Technology*, 32(7):3123–3128, 2018.

[16] Jacob Mayowa Owoyemi, Habeeb Olawale Zakariya, and Isa Olalekan Elegbede. Sustainable wood waste management in nigeria. *Environmental & Socio-economic Studies*, 4(3):1–9, 2016.

[17] E. Gallo, B. Schartel, D. Acierno, F. Cimino, and P. Russo. Tailoring the flame retardant and mechanical performances of natural fiber-reinforced biopolymer by multi-component laminate. *Composites Part B: Engineering*, 44(1):112–119, 2013.

[18] Keyang Lu, Robert H. White, Feng Fu, Junfeng Hou, Yisheng Zhang, Neil Gribbins, and Zhiyong Cai. Reinforced hybrid wood-aluminum composites with excellent fire performance. *Holzforschung*, 69(8):1027–1037, 2015.

[19] Peter Omoniyi, Adebayo Adekunle, Segun Ibitoye, Olalekan Olorunpomi, and Olatunji Abolusoro. Mechanical and microstructural evaluation of aluminium matrix composite reinforced with wood particles. *Journal of King Saud University - Engineering Sciences*, 2 2021.

[20] Hamideh Faridi and Akbar Arabhosseini. Application of eggshell wastes as valuable and utilizable products: A

review. *Research in Agricultural Engineering*, 64(2):104–114, 2018.
[21] Gabriele De Angelis, Laura Medeghini, Aida Maria Conte, and Silvano Mignardi. *Recycling of eggshell waste into low-cost adsorbent for Ni removal from wastewater*, volume 164. Elsevier Ltd, 2017.
[22] O. S. Olusesi and N. E. Udoye. Development and characterization of aa6061 aluminium alloy /clay and rice husk ash composite. *Manufacturing Letters*, 29:34–41, 2021.
[23] S. B. Hassan and V. S. Aigbodion. Effects of eggshell on the microstructures and properties of al–cu–mg/eggshell particulate composites. *Journal of King Saud University - Engineering Sciences*, 27(1):49–56, 2015.
[24] Shashi Prakash Dwivedi, Satpal Sharma, and Raghvendra Kumar Mishra. Synthesis and mechanical behaviour of green metal matrix composites using waste eggshells as reinforcement material. *Green Processing and Synthesis*, 5(3):275–282, 2016.
[25] Shrawan Kumar, Shashi Prakash Dwivedi, and Vijay Kumar Dwivedi. Synthesis and characterization of ball-milled eggshell and al2o3 reinforced hybrid green composite material. *Journal of Metals, Materials and Minerals*, 30(2):67–75, 2020.
[26] Irwin M. Hutten. Raw materials for nonwoven filter media. *Handbook of Nonwoven Filter Media*, pages 103–194, 1 2007.
[27] K N Satheeshan, B R Seema, and A V Meera Manjusha. Development of virgin coconut oil based body lotion. *The Pharma Innovation Journa*, 9(5):96–101, 2020.
[28] Husni Husin, Abubakar Abubakar, Suci Ramadhani, Cici Ferawati Br Sijabat, and Fikri Hasfita. Coconut husk ash as heterogenous catalyst for biodiesel production from cerbera manghas seed oil. *MATEC Web of Conferences*, 197:2–5, 2018.
[29] X. Bonneau, Irfan Haryanto, and Triyono Karsiwan. Coconut husk ash as a fertilizer for coconut palms on peat. *Experimental Agriculture*, 46(3):401–414, 2010.
[30] Rifki Husnul Khuluk, Ali Rahmat, Buhani, and Suharso. Removal of methylene blue by adsorption onto activated carbon from coconut shell (cocous nucifera l.). *Indonesian Journal of Science and Technology*, 4(2):229–240, 2019.
[31] Muhammad Fahmi Anuar, Yap Wing Fen, Mohd Hafiz Mohd Zaid, Khamirul Amin Matori, and Rahayu Emilia Mohamed Khaidir. The physical and optical studies of crystalline silica derived from the green synthesis of coconut husk ash. *Applied Sciences (Switzerland)*, 10(6), 2020.
[32] Ravi Butola, Chandra Pratap, Anurag Shukla, and R. S. Walia. Effect on the mechanical properties of aluminum-based hybrid metal matrix composite using stir casting method. *Materials Science Forum*, 969 MSF:253–259, 2019.
[33] Balasubramani Subramaniam, Balaji Natarajan, Balasubramanian Kaliyaperumal, and Samson Jerold Samuel Chelladurai. Investigation on mechanical properties of aluminium 7075 - boron carbide - coconut shell fly ash reinforced hybrid metal matrix composites. *China Foundry*, 15(6):449–456, 2018.
[34] Siva Sankara Raju and Gunji Srinivas Rao. Assessments of desirability wear behaviour on al-coconut shell ash - metal matrix composite using grey - fuzzy reasoning grade. *Indian Journal of Science and Technology*, 10(15):1–11, 2017.
[35] S. K.S. Hossain, Lakshya Mathur, and P. K. Roy. Rice husk/rice husk ash as an alternative source of silica in ceramics: A review. *Journal of Asian Ceramic Societies*, 6(4):299–313, 2018.
[36] Bhupinder Singh. *Rice husk ash*. Elsevier Ltd, 2018.
[37] Srikant Tiwari and M. K. Pradhan. Effect of rice husk ash on properties of aluminium alloys: A review. *Materials Today: Proceedings*, 4(2):486–495, 2017.
[38] J. Allwyn Kingsly Gladston, I. Dinaharan, N. Mohamed Sheriff, and J. David Raja Selvam. Dry sliding wear behavior of aa6061 aluminum alloy composites reinforced rice husk ash particulates produced using compocasting. *Journal of Asian Ceramic Societies*, 5(2):127–135, 2017.
[39] Sinae Song, Hong Baek Cho, and Hee Taik Kim. Surfactant-free synthesis of high surface area silica nanoparticles derived from rice husks by employing the taguchi approach. *Journal of Industrial and Engineering Chemistry*, 61:281–287, 2018.
[40] Ganabpaty Thiagarajan, Noradila Abdul Latif, Nurul Farahin, and Mohd Joharudin. Advanced research in natural fibers preliminary study on crystallinity of rice husk ash reinforcement for metal matrix composite. *Advanced Research in Natural Fibers*, 2(1):21–24, 2020.
[41] S. D. Saravanan and M. Senthil Kumar. Effect of mechanical properties on rice husk ash reinforced aluminum alloy (alsi10mg) matrix composites. *Procedia Engineering*, 64:1505–1513, 2013.
[42] Mohd Bilal Naim Shaikh, Sufian Raja, Mukhtar Ahmed, Mohammed Zubair, Adnan Khan, and Mohammed

Ali. Rice husk ash reinforced aluminium matrix composites: fabrication, characterization, statistical analysis and artificial neural network modelling. *Materials Research Express*, 6(5):056518, feb 2019.

[43] Sumit Saini, Shankar Singh, Kulwant Singh, and Abhishek Singh. Some studies into weldability of rice husk ash aluminium matrix composites using tig welding. *Materials Today: Proceedings*, 24:298–307, 2020.

[44] Isaac Dinaharan, Kumaravel Kalaiselvan, and Nadarajan Murugan. Influence of rice husk ash particles on microstructure and tensile behavior of aa6061 aluminum matrix composites produced using friction stir processing. *Composites Communications*, 3(January):42–46, 2017.

[45] A. O. Inegbenebor, C. A. Bolu, P. O. Babalola, A. I. Inegbenebor, and O. S.I. Fayomi. Aluminum Silicon Carbide Particulate Metal Matrix Composite Development Via Stir Casting Processing. *Silicon*, 10(2):343–347, 2018.

[46] The Aluminium Association. International Alloy Designations and Chemical Composition Limits for Wrought Aluminum and Wrought Aluminum Alloys With Support for On-line Access From: Aluminum Extruders Council Use of the Information. *The Aluminum Association, Arlington, Virginia*, 5(Enero 2015):31, 2015.

[47] Yu Wang, Langjie Zhu, Guodong Niu, and Jian Mao. Conductive Al Alloys: The Contradiction between Strength and Electrical Conductivity. *Advanced Engineering Materials*, 23(5):1–22, 2021.

[48] S. A.Mohan Krishna, T. N. Shridhar, and L. Krishnamurthy. Microstructural characterization and investigation of thermal conductivity behaviour of al 6061-sic-gr hybrid metal matrix composites. *Indian Journal of Engineering and Materials Sciences*, 23(4):207–222, 2016.